Journal of Marine Science and Technology

Volume 23 | Issue 2 Article 5

# NONLINEAR BREAKER CHARACTERISTICS AND IMPULSE ON A SLOPING BOTTOM

Wen-Jer Tseng
*Department of Civil Engineering and Geomatics, Cheng Shiu University, Kaohsiung City, Taiwan, R.O.C.*,
jwj@gcloud.csu.edu.tw



Recommended Citation
Tseng, Wen-Jer (2015) "NONLINEAR BREAKER CHARACTERISTICS AND IMPULSE ON A SLOPING BOTTOM," *Journal of Marine Science and Technology*: Vol. 23 : Iss. 2 , Article 5.
DOI: 10.6119/JMST-014-0416-3
Available at: https://jmstt.ntou.edu.tw/journal/vol23/iss2/5

Journal of Marine Science and Technology, Vol. 23, No. 2, pp. 172-182 (2015)
DOI: 10.6119/JMST-014-0416-3

# NONLINEAR BREAKER CHARACTERISTICS AND IMPULSE ON A SLOPING BOTTOM

Wen-Jer Tseng

Key words: Eulerian system, Lagrangian system, breaker characteristics, breaker impulse.

## ABSTRACT

This paper presents an experimental and theoretical investigation of nonlinear surface-wave propagation over a sloping bed. First, a second-order analytical solution for nonlinear surface-wave propagation over a sloping bed is derived using a perturbation method for the bottom slope $\alpha$ and the wave steepness $\varepsilon$ in an Eulerian system. Then, by transforming the flow field solution from an Eulerian system into a Lagrangian system, more accurate wave profiles are determined. New theoretical breaker characteristics and breaker impulses are derived using the kinematic stability parameter. Subsequently, a series of experiments to measure breaker characteristics and the breaker impulse are conducted in a wave tank. The theoretical solutions are compared with both the present experimental data and previously published experimental results. The results reveal that the analytical solution can reasonably describe the wave breaking phenomenon. In this paper, a new theoretical solution for the breaker characteristics and impulses is provided, which is proven to be a useful approach for follow-up studies to predict breaker characteristics and impulses.

## I. INTRODUCTION

Because of changes in water depth, waves are affected by the bottom when the depth is shorter than half of a wave length; waves shoal in the propagation process from deep water to shallow water. Moreover, wave heights increase and the wave profile becomes more skewed and asymmetric (Elgar and Guza, 1985) due to nonlinear effects. The celerity is reduced; hence, the particle velocity of the wave crest is faster than the celerity, and the wave subsequently breaks. Breaking waves release substantial energy and supply a large impact force that damages coastal structures, such as breakwaters, and drives sediment transport along/across the nearshore region. Therefore, breaker characteristics must be quantified to reliably predict sediment transport and structural design in coastal regions. Most investigators have discussed and utilized formulas from experimental studies. For example, Street and Camfield (1966), Tang (1966), Lé Méhauté and Koh (1967), Galvin (1968), Saeki et al. (1971), Goda (1970, 2004), Sunamura and Horikawa (1974), Sunamura (1980, 1983), Ogawa and Shuto (1984), Seyama and Kimura (1988), Hansen (1990), and Rattanapitikon and Shibayama (2000) have proposed empirical formulas or semi-empirical formulas for the breaker height and breaker depth as a function of the deep wave height, wave steepness, and bottom slope in accordance with experiments or reliable field data. Chang (1999), Gotoh and Sakai (1999), Hsieh et al. (2007) and Hsieh et al. (2008) studied breaker characteristics using numerical simulations; Deo et al. (2003) studied the same topic using neural networks and experimental results. Furthermore, Iwagaki et al. (1974), Hubert et al. (1997), Ting et al. (2002), Tsai et al. (2005), and Hsiao et al. (2008) utilized experimental data to examine several empirical formulas or characteristics of breaking waves. The major drawbacks of the above studies are that they can only derive the breaker height or breaker depth and provide the location of the breaking wave at the time in which it breaks; however, they cannot completely describe the wave deformation process and the related flow field. Moreover, breaking waves induce large impact forces and substantial breaker impulses in a relatively short period of time, which may result in the subsequent displacement and damage on a caisson breakwater. Therefore, breaker characteristics and impulses must be quantified to improve the design of coastal protection structures.

Biesel (1952) suggested a plausible approximation method to account for normal incident waves propagating on a sloping plane where the bottom slope was first considered as a perturbation parameter in the velocity potential; however, wave breaking and nonlinear effects were not treated in his study. Furthermore, details on the derivation of the formula are not provided. Chen and Tang (1992), Hsu et al. (2001) and Chen et al. (2005, 2006) have extended Biesel's theory. However, wave impulses remains missing in an explicit analytical solution for breaking waves on a gently sloping bottom.

In this paper, a nonlinear analysis is given by perturbing

*Paper submitted 11/14/13; revised 12/31/13; accepted 04/16/14. Author for correspondence: Wen-Jer Tseng (e-mail: jwj@gcloud.csu.edu.tw).*
*Department of Civil Engineering and Geomatics, Cheng Shiu University, Kaohsiung City, Taiwan, R.O.C.*

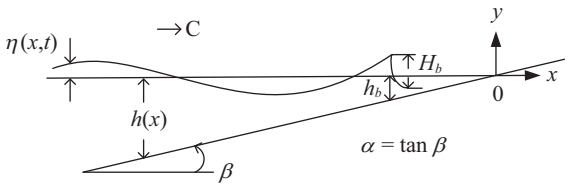


**Fig. l. Schematic of a surface wave propagating on a gently sloped bottom.**

the second order solution for a bottom slope $\alpha$ and/or wave steepness $\varepsilon$ in an Eulerian system. Then, the wave breaking profile is determined by transforming the Eulerian system into a Lagrangian system. Next, the breaker height, the breaker depth and the breaker impulse are calculated using kinematic stability parameter. Subsequently, a laboratory experiment is conducted to validate the theoretical results on a sloping bottom. Finally, the theoretical solutions are compared with both the present experiment and previously published experimental results (Fig. 6 to Fig. 9).

## II. MATHEMATICAL FORMULATION

A two-dimensional Cartesian $x$-$y$ coordinate system is used to describe a surface wave propagating toward a gentle uniformly sloped bottom (Fig. l). The negative $x$-axis is directed seaward, while the positive y-axis is positioned vertically from the still water level; the sea bottom is at $y = -h = \alpha x$, in which $\alpha$ denotes the bottom slope (Chen et al., 2005; Li et al., 2013).

Here, $\beta$ is the bottom inclination angle, $\alpha$ (= tan $\beta$) is the bottom slope, $\eta(x, t)$ is the water surface elevation, $C$ is the celerity, $h(x)$ is the water depth, $H_b$ is the breaker height and $h_b$ is the breaker depth.

By assuming that the flow motion is irrotational, incompressible and inviscid, the second-order governing equations and boundary conditions can be derived for the bottom slope $\alpha$ and/or the wave steepness $\varepsilon$ ($H_o/L_o$), where $H_o$ is the wave height and $L_o$ is the deep water wave or incident wave length. To describe the irrotational motion of an inviscid and incompressible fluid, a velocity potential $\phi(x, y, t)$ is introduced and the horizontal and vertical velocities are given by

$$u = \frac{\partial \phi}{\partial x}, v = \frac{\partial \phi}{\partial y}, \vec{V} = u\vec{i} + v\vec{j}. \tag{1}$$

The velocity potential $\phi(x, y, t)$ is harmonic with respect to $x$ and $y$ and satisfies the continuity equation, which leads to the following Laplace equation:

$$\nabla^2 \phi = \frac{\partial^2 \phi}{\partial x^2} + \frac{\partial^2 \phi}{\partial y^2} = 0. \tag{2}$$

The wave motion that is described above must respectively satisfy the following boundary conditions at the bottom and the free surface:

(1) On an immovable and impermeable sloping plane with an inclination $\beta$ relative to the horizon, represented by $f(x, y) = y + h = y - \alpha x = 0$, the no-flux bottom boundary condition gives

$$\nabla \phi \cdot \vec{n} = \nabla \phi \cdot \frac{\nabla f}{|\nabla f|} = \frac{-\alpha \phi_x + \phi_y}{\sqrt{1+\alpha^2}} = 0, \ y = -h, \text{ and } x \le 0,$$

or simply

$$\frac{\partial \phi}{\partial y} - \alpha \frac{\partial \phi}{\partial x} = 0, \ y = -h. \tag{3}$$

(2) The dynamic and kinematic free surface boundary conditions are

$$\phi_t + (\nabla \phi)^2 / 2 + g\eta = 0, \ y = \eta, \tag{4}$$

$$\phi_y = d\eta / dt, \ y = \eta. \tag{5}$$

The total differential, i.e., D/Dt, of Eq. (4) and using Eq. (5) gives

$$\phi_{tt} + g\phi_y + [(\nabla \phi)^2]_t + \nabla \phi \cdot \nabla (\nabla \phi)^2 / 2 = 0, \ y = \eta. \tag{6}$$

For a gentle sloping bottom with slope $\alpha$, Eqs. (2) to (6) can be solved in order; the solution is provided in the following section.

## III. ASYMPTOTIC SOLUTION ANALYSIS

In this section, an explicit expression for the velocity potential of the wave field is first derived as a function of the bottom slope $\alpha$ and the wave steepness $\varepsilon$ to the second order in an Eulerian coordinate system. Then, the wave profile and the velocity components are transformed into a Lagrangian system. Finally, in the subsequent section, the kinematic stability parameter is introduced; theoretical breaker characteristics and the breaker impulse are derived. The detailed computation is given below.

To solve the boundary value problem described in Eqs. (2) to (6), it is assumed that the relevant physical quantities can be expanded using a double power series of the wave steepness $\varepsilon$ and the bottom slope $\alpha$. Therefore, the velocity potential $\phi$ and the water surface elevation $\eta$ can be expanded as

$$\phi = \sum_{m=1}^{\infty} \sum_{n=0}^{\infty} \varepsilon^m \alpha^n f_{mn}(x, y, t) = \varepsilon (f_{10} + \alpha f_{11} + \alpha^2 f_{12} + ...)$$

$$+ \varepsilon^2 (f_{20} + \alpha f_{21} + ...) + ....., \tag{7}$$

$$\eta = \sum_{m=1}^{\infty}\sum_{n=0}^{\infty} \varepsilon^m \alpha^n \eta_{mn} = \varepsilon(\eta_{10} + \alpha\eta_{11} + \alpha^2\eta_{12} + ...) + \varepsilon^2(\eta_{20} + \alpha\eta_{21} + ...) + ..... . \quad (8)$$

Consider a two-dimensional monochromatic wave propagating normal to a gently sloped bottom from deep water to shallow water, the lowest order solution for the velocity potential and the surface elevation (Keller, 1958; Chen and Tang 1992) are assumed to be

$$\varepsilon f_{10} = -a\frac{g\cosh k(h+y)}{\sigma\cosh kh}\sin(\sigma t - \int kdx) \quad (9)$$

and

$$\varepsilon\eta_{10} = a\cos(\sigma t - \int kdx) . \quad (10)$$

Here, $\sigma$ is the angular frequency and $k$ is the wave number. Because the bottom slope $\alpha = -d(h(x))/dx = -h_x$ is the perturbation parameter and both the wave amplitude factor $a$ and the wave number $k$ are functions of $x$, the n-th differentiation of both $a$ and $k$ with respect to $x$ can be determined up to the order of $\alpha^n$, or

$$\begin{cases} \dfrac{d^n a}{dx^n} = O(\alpha^n), \\ \dfrac{d^n k}{dx^n} = O(\alpha^n). \end{cases} \quad (11)$$

Using Eq. (7) and Eq. (9), we can derive the following:

$$\phi_x = \frac{g}{\sigma}\{[-a_x + a(hk)_x \tanh kh]\frac{\cosh k(h+y)}{\cosh kd} - a[k_x(h+y) + kh_x]\frac{\sinh k(h+y)}{\cosh kh}\}\sin(\sigma t - \int kdx) + \frac{g}{\sigma}(ak)\frac{\cosh k(h+y)}{\cosh kh} \times \cos(\sigma t - \int kdx) + \varepsilon\alpha f_{11x} + \varepsilon\alpha^2 f_{12x} + ....., \quad (12)$$

$$\phi_{xx} = \frac{g}{\sigma}\{-a_{xx} + [2a_x(kh)_x + a(kh)_{xx}]\tanh kh + (1 - 2\tanh^2 kh)a[(kh)_x]^2 - a[k_x(h+y) + kh_x]^2\} \times [\frac{\cosh k(h+k)}{\cosh kh}]\sin(\sigma t - \int kdx) + \frac{g}{\sigma}\{[2a_x + 2a(kh)_x \tanh kh][k_x(h+y) + kh_x] - a[k_x(h+y) + kh_x]_x\}[\frac{\sinh k(h+y)}{\cosh kh}]\sin(\sigma t - \int kdx) + \frac{g}{\sigma}\{[2a_x k - 2ak(kh)_x \tanh kd + ak_x][\frac{\cosh k(h+y)}{\cosh kh}] + 2ak[k_x(h+y) + kd_x][\frac{\sinh k(h+y)}{\cosh kh}]\}\cos(\sigma t - \int kdx) + \frac{g}{\sigma}(ak^2)\frac{\cosh k(h+y)}{\cosh kh}\sin(\sigma t - \int kdx) + \varepsilon\alpha f_{11xx} + \varepsilon\alpha^2 f_{12xx} + ....., \quad (13)$$

$$\phi_y = -\frac{g}{\sigma}(ak)\frac{\sinh k(h+y)}{\cosh kh}\sin(\sigma t - \int kdx) + \varepsilon\alpha f_{11y} + \varepsilon\alpha^2 f_{12y} + ....., \quad (14)$$

$$\phi_{yy} = -\frac{g}{\sigma}(ak^2)\frac{\cosh k(h+y)}{\cosh kh}\sin(\sigma t - \int kdx) + \varepsilon\alpha f_{11yy} + \varepsilon\alpha^2 f_{12yy} + ....., \quad (15)$$

and

$$\phi_{tt} = ag\sigma\frac{\cosh k(h+y)}{\cosh kh}\sin(\sigma t - \int kdx) + \varepsilon\alpha f_{11tt} + \varepsilon\alpha^2 f_{12tt} + ..... . \quad (16)$$

Then, by substituting Eqs. (12) to (16) into Eq. (6), using the Taylor expansion with respect to $y = 0$ for values calculated at $y = \eta$ and collecting the terms with the same order in $\varepsilon^m\alpha^n$, Eq. (6) becomes (Chen et al., 2005)

$$-\frac{g}{\sigma}a(gk\tanh kh - \sigma^2)\sin(\sigma t - \int kdx) + \varepsilon\alpha(gf_{11y} + f_{11tt})_{y=0} + \varepsilon\alpha^2(gf_{12y} + f_{12tt})_{y=0} + \varepsilon^2(gf_{20y} + f_{20tt} + g\eta_{10}f_{10yy} + \eta_{10}f_{10ytt} + 2f_{10x}f_{10xt} + 2f_{10y}f_{10yt})_{y=0} ..... = 0. \quad (17)$$

Similarly, the bottom boundary condition from Eq. (3) becomes

$$(\varepsilon\alpha f_{11y} + \varepsilon^2 f_{20y})_{y=-h} - \alpha\frac{g}{\sigma}(\frac{ak}{\cosh kh})\cos(\sigma t - \int kdx) + \alpha\frac{g}{\sigma}[\frac{a_x - a(kh)_x \tanh kh}{\cosh kh}]\sin(\sigma t - \int kdx) + ..... = 0. \quad (18)$$

By applying Eq. (11) and the lowest two orders of the combined free surface boundary condition, Eq. (17) gives the linear dispersion relation and the constraints for $f_{11}$ and $f_{12}$ as

$$\sigma^2 = gk \tanh kh, \tag{19}$$

$$(gf_{11y} + f_{11tt})_{y=0} = 0, \tag{20}$$

$$(gf_{12y} + f_{12tt})_{y=0} = 0. \tag{21}$$

Similarly, the lowest two orders of the bottom boundary condition from Eq. (18) give

$$[(\varepsilon f_{11})_y]_{y=-h} = \frac{g}{\sigma}(\frac{ak}{\cosh kh})\cos(\sigma t - \int kdx). \tag{22}$$

Based on this condition, the lowest order fundamental mode is

$$\varepsilon f_{11}(x, y, t) = A_1(x, y)\frac{\cos(\sigma t - \int kdx)}{\cosh kh}. \tag{23}$$

Here,

$$(A_{1y})_{y=-h} = (\frac{gak}{\sigma}), \tag{24}$$

and $A_1$ varies with both $x$ and $y$.

Using the same assumption for $a$ and $k$, the differentiation of $A_1$ with respect to is of order $\alpha^n$:

$$\frac{\partial^n A_1}{\partial x^n} = O(\alpha^n). \tag{25}$$

Substituting $f_{11}$ into the $O(\varepsilon\alpha)$ terms of the Laplace equation, $A_1$ can be obtained as

$$A_1 = \{\frac{g}{\alpha\sigma}[-a_x + a(kh)_x \tanh kh](h+y) + D_1\}\sinh k(h+y)$$

$$-\{\frac{g}{\alpha\sigma}[\frac{1}{2}ak_x(h+y)^2 + akh_x(h+y)] + D_2\}\cosh k(h+y), \tag{26}$$

where $D_1$ and $D_2$ depend only on $x$. According to Eq. (24) and the fact that $h_x = (-\alpha)$, $D_1$ is zero.

By substituting $A_1$ into Eq. (23), the velocity potential perturbation $\varepsilon f_{11}$ can be expressed as

$$\varepsilon f_{11} = \frac{g}{\alpha\sigma}\{[-a_x + a(kh)_x \tanh kh][\frac{\sinh k(h+y)}{\cosh kh}](h+y)$$

$$-[\frac{1}{2}ak_x(h+y)^2 + akh_x(h+y) + \frac{\alpha\sigma}{g}D_2]$$

$$\times[\frac{\cosh k(h+y)}{\cosh kh}]\}\cos(\sigma t - \int kdx). \tag{27}$$

Then, by substituting it into the constraint derived from the free surface boundary condition, i.e., Eq. (20), we obtain

$$\frac{a_x}{a} = -\frac{[\tanh kh + (kh)\operatorname{sech}^2 kh]_x}{2[\tanh kh + (kh)\operatorname{sech}^2 kh]}. \tag{28}$$

By integrating Eq. (28) with respect to $x$, the following amplitude parameter is obtained:

$$a = \frac{a_o}{(D \tanh kh)^{1/2}}. \tag{29}$$

where $D = [1 + (2kh/\sinh 2kh)]$ and $a_o$ is the amplitude of the deep water wave.

Then, using the definition of the bottom slope, i.e., $h_x = (-\alpha)$ and the condition $f_{11} \to 0$ as $h \to \infty$, $D_2 = 0$ and $\varepsilon\alpha f_{11}$ can be written as

$$\varepsilon\alpha f_{11} = -\alpha\frac{g}{\sigma}\{a\frac{k(h+y)\sinh k(h+y)}{D^2 \tanh kh} + a[\frac{k^2(h+y)^2}{D\sinh 2kh}$$

$$-k(h+y)]\cosh k(h+y)\}[\frac{\cos(\sigma t - \int kdx)}{\cosh kh}]. \tag{30}$$

Eq. (30) represents the $O(\varepsilon\alpha)$ term of the velocity potential $\phi$. To study breaking waves, nonlinear terms of order $\varepsilon^2$ must be considered. Following the first-order approximation, the second-order governing equation and boundary conditions are given as

$$(\varepsilon^2 f_{20})_{xx} + (\varepsilon^2 f_{20})_{yy} = 0, \tag{31}$$

$$(\varepsilon^2 f_{20})_{tt} + g(\varepsilon^2 f_{20})_y = \frac{3}{2}\frac{a^2 g^2 k^2}{\sigma}(1 - \tanh^2 kh)$$

$$\times \sin\left[2(\sigma t - \int kdx)\right], \quad y = 0, \tag{32}$$

$$(\varepsilon^2 f_{20})_y = 0, \quad y = -h. \tag{33}$$

A general solution for $\varepsilon^2 f_{20}$ that satisfies both the Laplace equation and the boundary conditions is assumed to follow a series form:

$$(\varepsilon^2 f_{20}) = \sum_{r=1}^{\infty} A_{2r}\frac{\cosh\left[rk(h+y)\right]}{\cosh(rkh)}\sin\left[r(\sigma t - \int kdx)\right]. \tag{34}$$

By substituting Eq. (34) into Eq. (32), we obtain

$$\sum_{r=1}^{\infty}\{[-r^2\sigma^2 A_{2r} + rgkA_{2r}\tanh(rkh)]\sin[r(\sigma t - \int kdx)]\}$$

$$= \frac{3}{2}\frac{a^2 g^2 k^2}{\sigma}(1 - \tanh^2 kh)\sin\left[2(\sigma t - \int kdx)\right].$$

Then, the following is obtained using the orthogonality of trigonometric functions:

$$A_{22} = -\frac{3}{8}a^2\sigma(\frac{\cosh(2kh)}{\sinh^4 kh}),\ A_{21} = 0 \text{ and } A_{2m} = 0\ (m \geq 3),$$

Eq. (34) is then reduced to

$$\varepsilon^2 f_{20} = -\frac{3}{8}a^2\sigma[\frac{\cosh[2k(h+y)]}{\sinh^4 kh}]\sin[2(\sigma t - \int kdx)]. \quad (35)$$

Other $O(\varepsilon^2)$ terms, such as $f_{21}$ and $f_{22}$, are negligible for small $\alpha$. Therefore, these terms are not shown in the following discussion. The complete solution to the second-order equation in terms of the wave steepness with a small bottom slope can be written as

$$\begin{aligned}\phi &= \varepsilon f_{10} + \varepsilon\alpha f_{11} + \varepsilon^2 f_{20}\\ &= -a\frac{g}{\sigma}\frac{\cosh k(h+y)}{\cosh kh}\sin(\sigma t - \int kdx)\\ &\quad - \alpha a\frac{g}{\sigma}\{\frac{k(h+y)\sinh k(h+y)}{D^2\tanh kh} + [\frac{k^2(h+y)^2}{D\sinh 2kh}\\ &\quad - k(h+y)]\cosh k(h+y)\}\frac{\cos(\sigma t - \int kdx)}{\cosh kh}\\ &\quad - \frac{3}{8}a^2\sigma\frac{\cosh[2k(h+y)]}{\sinh^4 kh}\sin[2(\sigma t - \int kdx)]. \end{aligned} \quad (36)$$

This Eulerian solution is transformed into a Lagrangian system to derive the deformation of the wave profile, the breaker criteria, and the breaker impulse; the details are discussed in the following section.

## IV. BREAKING WAVE AND BREAKER IMPULSE

### 1. Wave Impulse for a Uniform Depth

Because the bottom is uniform before waves enter a gently sloped bottom, Eq. (36) can be reduced to

$$\phi = -\frac{g}{\sigma}a_i\frac{\cosh k(h+y)}{\cosh kh}\sin(\sigma t - \int kdx). \quad (37)$$

The pressure can be calculated from Brenoulli's equation:

$$\phi_t + \frac{(u_e^2 + v_e^2)}{2} + \frac{P}{\rho} + gy = 0. \quad (38)$$

The dynamic pressure at a fixed position can then be obtained as follows by assuming linearity:

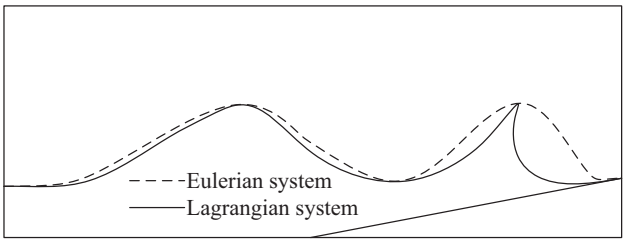


**Fig. 2. Comparison of wave profiles between Lagrangian and Eulerian coordinates.**

$$P_d(y,t) = \rho g a_i\frac{\cosh k(h+y)}{\cosh kh}\cos(\sigma t). \quad (39)$$

Then, the positive wave impulse per unit width $I_t$ can be obtained as follows:

$$\begin{aligned} I_t &= 2\int_0^{T_i/4}\int_0^{a_i} P_d(y,t)\,dydt\\ &= (\rho a_i C_i/k)(\frac{2\sinh k(h+a_i)}{\sinh kh} - 2). \end{aligned} \quad (40)$$

Here $C_i$ is the wave celerity, i.e., $C_i = (gT_i/2\pi)\tanh kh$, $a_i$ is the wave amplitude, $T_i$ is the wave period, $\rho$ is the density of water and the subscript $i$ denotes the incident wave or the deep water wave.

### 2. Wave Deformation

As a wave reaches its limit, the crest is fully developed as a summit and becomes highly asymmetric, which can be described using a Lagrangian coordinate system; the Lagrangian system captures details that cannot be captured in an Eulerian system. Hence, the motion described in the Lagrangian system is close to reality (Chen et al., 2004).

The Eulerian and Lagrangian wave profiles prior to the wave breaking as the wave propagates over a gently sloped bottom $(0 < \alpha \leq 1/10)$ are demonstrated in Fig. 2.

The horizontal and vertical Eulerian velocity components of the fluid particle, i.e., $u_e = \partial\phi/\partial x$ and $v_e = \partial\phi/\partial y$, can be derived according to the velocity potential given in the previous section. As a wave shoals, the wave form becomes asymmetric and the particle motion can be obtained by the transformation between Eulerian and Lagrangian coordinates. The Lagrangian velocity may be estimated from the Eulerian velocity according to Chen et al. (2006)

$$\begin{aligned}\vec{V}_L(\vec{a},t) &= \vec{V}_E[\vec{a} + \int_{t_0}^{t}\vec{V}_L(\vec{a},t')\,dt', t]\\ &= \vec{V}_E(\vec{a},t) + \int_{t_0}^{t}\vec{V}_L(\vec{a},t')\,dt'\cdot\nabla_{\vec{a}}\vec{V}_E(\vec{a},t) + H.O.T. \end{aligned}$$

Here the Eulerian (Lagrangian) velocity is $\vec{V}_E = [u_e, v_e]$

($\vec{V}_L = [u_\ell, v_\ell]$) and $\vec{a}$ is the position of a fluid particle at time $t = t_0$. Then, the Eulerian motions can be transferred into the Lagrangian system according to the fluid particle trajectory; the corresponding velocity components, namely, $u_\ell$ and $v_\ell$, are

$$\begin{aligned} u_\ell &= u_e + (\int^t u_e dt)\frac{\partial u_e}{\partial x} + (\int^t v_e dt)\frac{\partial u_e}{\partial y} \\ &= a\sigma \frac{\cosh k(h+y)}{\sinh kh}\cos(\sigma t - \int kdx) - \alpha a \frac{\sigma}{\sinh kh} \\ &\quad \times [\frac{\cosh k(h+y)}{D^2 \tanh kh} + \frac{k(h+y)\sinh k(h+y)}{D^2 \tanh kh} \\ &\quad + \frac{2k(h+y)\sinh k(h+y)}{D\sinh 2kh} + \frac{k^2(h+y)^2}{D\sinh 2kh} \\ &\quad \times \cosh k(h+y) - \sinh k(h+y) - k(h+y) \\ &\quad \times \cosh k(h+y)]\sin(\sigma t - \int kdx) + \frac{3}{4}a^2 k\sigma \\ &\quad \times \frac{\cosh 2k(h+y)}{\sinh^4 kh}\cos 2(\sigma t - \int kdx) + a^2 k\sigma \\ &\quad \times \frac{1}{2\sinh^2 kh}\left[\cosh 2k(h+y) - \cos 2(\sigma t - \int kdx)\right], \end{aligned} \tag{41}$$

$$\begin{aligned} v_\ell &= v_e + (\int^t u_e dt)\frac{\partial v_e}{\partial x} + (\int^t v_e dt)\frac{\partial v_e}{\partial y} \\ &= -a\sigma \frac{\sinh k(h+y)}{\sinh kh}\sin(\sigma t - \int kdx) - \alpha a \frac{\sigma}{\sinh kh} \\ &\quad \times [\frac{\sinh k(h+y)}{D^2 \tanh kh} + \frac{k(h+y)\cosh k(h+y)}{D^2 \tanh kh} \\ &\quad + \frac{2k(h+y)\cosh k(h+y)}{D\sinh 2kh} + \frac{k^2(h+y)^2}{D\sinh 2kh} \\ &\quad \times \sinh k(h+y) - \cosh k(h+y) - k(h+y) \\ &\quad \times \sinh k(h+y)]\cos(\sigma t - \int kdx) - \frac{3}{4}a^2 k\sigma \\ &\quad \times \frac{\sinh 2k(h+y)}{\sinh^4 kh} \times \sin 2(\sigma t - \int kdx). \end{aligned} \tag{42}$$

Furthermore, the displacement components $X$ and $Y$ of the fluid particle with an initial average position of $(x, y)$ are obtained via direct integration to obtain

$$\begin{aligned} X &= \int^t u_\ell \, dt \\ &= a\frac{\cosh k(h+y)}{\sinh kh}\sin(\sigma t - \int kdx) + \alpha \frac{a}{\sinh kh} \\ &\quad \times [\frac{\cosh k(h+y)}{D^2 \tanh kh} + \frac{k(h+y)\sinh k(h+y)}{D^2 \tanh kh} \\ &\quad + \frac{2k(h+y)\sinh k(h+y)}{D\sinh 2kh} + \frac{k^2(h+y)^2\cosh k(h+y)}{D\sinh 2kh} \\ &\quad - \sinh k(h+y) - k(h+y)\cosh k(h+y)]\cos(\sigma t - \int kdx) \\ &\quad + a^2 k \frac{1}{\sinh^2 kh}\left[-\frac{1}{4} + \frac{3}{8}\frac{\cosh 2k(h+y)}{\sinh^2 kh}\right] \\ &\quad \times \sin\left[2(\sigma t - \int kdx)\right] + \frac{1}{2}a^2 k\sigma \frac{\cosh 2k(h+y)}{\sinh^2 kh}t, \end{aligned} \tag{43}$$

$$\begin{aligned} Y &= \int^t v_\ell \, dt \\ &= a\frac{\sinh k(h+y)}{\sinh kh}\cos(\sigma t - \int kdx) - \alpha \frac{a}{\sinh kh} \\ &\quad \times [\frac{\sinh k(h+y)}{D^2 \tanh kh} + \frac{k(h+y)\cosh k(h+y)}{D^2 \tanh kh} \\ &\quad + \frac{2k(h+y)\cosh k(h+y)}{D\sinh 2kh} + \frac{k^2(h+y)^2\sinh(h+y)}{D\sinh 2kh} \\ &\quad - \cosh k(h+y) - k(h+y)\sinh k(h+y)] \\ &\quad \times \sin(\sigma t - \int kdx) + \frac{3}{8}a^2 k\frac{\sinh 2k(h+y)}{\sinh^4 kh} \\ &\quad \times \cos\left[2(\sigma t - \int kdx)\right]. \end{aligned} \tag{44}$$

By substituting $y = 0$ into Eq. (43) and Eq. (44), the water particle displacement on the free surface, i.e., $\xi$ and $\varsigma$, can be given as

$$\begin{aligned} \xi &= x + (X)_{y=0} \\ &= x + \frac{a}{\tanh kh}\sin(\sigma t - \int kdx) + \alpha a[\frac{1 + kh\tanh kh}{D^2 \tanh^2 kh} \\ &\quad + \frac{2kh + k^2h^2\coth kh}{D\sinh 2kh} - kh\coth kh - 1] \\ &\quad \times \cos(\sigma t - \int kdx) + a^2 k\frac{1}{\sinh^2 kh}[-\frac{1}{4} + \frac{3}{8}\frac{\cosh 2kh}{\sinh^2 kh}] \\ &\quad \times \sin[2(\sigma t - \int kdx)] + \frac{1}{2}a^2 k\sigma \frac{\cosh 2kh}{\sinh^2 kh}t, \end{aligned} \tag{45}$$

$$\begin{aligned} \varsigma &= (Y)_{y=0} \\ &= a\cos(\sigma t - \int kdx) - \alpha a[\frac{kh + \tanh kh}{D^2 \tanh^2 kh} \\ &\quad + \frac{2kh\coth kh + k^2h^2}{D\sinh 2kh} - \coth kh - kh] \end{aligned}$$

$$\times \sin(\sigma t - \int kdx) + \frac{3}{8} a^2 k \frac{\sinh 2kh}{\sinh^4 kh}$$

$$\times \cos[2(\sigma t - \int kdx)], \quad (46)$$

where ($\xi$, $\varsigma$) is the position of the fluid particle on the free surface.

## 3. Breaker Characteristics and the Breaker Impulse

The increase in wave height is due to the fact that shoaling becomes depth-limited as the wave propagates into shallow waters. Simultaneously, the celerity is reduced. Moreover, the particle velocity of the wave crest is faster than the wave celerity; therefore, the wave begins breaking. To describe the breaking wave mechanism, the kinematic stability parameter ($K.S.P.$) is introduced; the breaker criterion is

$$K.S.P. = \frac{u_{ob}}{C} = 1 , \quad (47)$$

where $C$ is celerity and $u_{ob}$ is the horizontal velocity of the particle at the wave crest.

According to Eq. (29), the breaking amplitude parameter $a_b$ can be written as

$$a_b = \frac{a_o}{(D_b \tanh k_b h_b)^{1/2}} , \quad (48)$$

where $D_b = [1 + (2k_b h_b / \sinh 2k_b h_b)]$ and the subscript $b$ denotes the breaking condition.

Up to the breaking point, the linear dispersion relation is still valid; therefore,

$$\sigma^2 = g k_b \tanh k_b h_b , \quad (49)$$

where $\sigma = k_b C_b$, $k_b$ and $C_b$ are the wave number and celerity, respectively, of the breaking wave, and $h_b$ is the breaker depth.

The Lagrangian velocities $u_\ell$ and $v_\ell$ evaluated at $y = 0$ can be simplified to

$$(u_\ell)_o = (u_{\ell 1})_o \cos(\sigma t - \int kdx) + (u_{\ell 2})_o \sin(\sigma t - \int kdx)$$

$$+ (u_{\ell 3})_o \cos\left[2(\sigma t - \int kdx)\right] + a^2 k \sigma \frac{\cosh 2kh}{2\sinh^2 kh}, \quad (50)$$

$$(v_\ell)_o = (v_{\ell 1})_o \sin(\sigma t - \int kdx) + (v_{\ell 2})_o \cos(\sigma t - \int kdx)$$

$$+ (v_{\ell 3})_o \sin\left[2(\sigma t - \int kdx)\right], \quad (51)$$

where

$$(u_{\ell 1})_o = \left(\frac{\sigma a}{\tanh kh}\right), \quad (52)$$

$$(u_{\ell 2})_o = -\alpha\sigma a\left[\frac{1 + kh \tanh kh}{D^2 \tanh^2 kh} + \frac{2kh + k^2 h^2 \coth kh}{D \sinh 2kh}\right.$$

$$\left. - kh \coth kh - 1\right], \quad (53)$$

$$(u_{\ell 3})_o = a^2 k \sigma \frac{1}{\sinh^2 kh}\left[-\frac{1}{2} + \frac{3}{4}\frac{\cosh 2kh}{\sinh^2 kh}\right], \quad (54)$$

$$(v_{\ell 1})_o = (-\sigma a) , \quad (55)$$

$$(v_{\ell 2})_o = -\alpha\sigma a\left[\frac{kh + \tanh kh}{D^2 \tanh^2 kh} + \frac{2kh \coth kh + k^2 h^2}{D \sinh 2kh}\right.$$

$$\left. - \coth kh - kh\right], \quad (56)$$

and

$$(v_{\ell 3})_o = -\frac{3}{4} a^2 k \sigma \frac{\sinh 2k(h + y)}{\sinh^4 kh} . \quad (57)$$

The breaker condition is defined by taking the extreme value of the horizontal velocity, i.e.,

$$\frac{\partial (u_\ell)_o}{\partial t} = 0 . \quad (58)$$

The phase angle of the breaking wave $\theta_b = (\sigma t - \int kdx)_b$ can be solved. Moreover, this condition also implies that the water surface elevation $\varsigma$ has an extreme value. Henceforth, the phase angle of the breaking wave is denoted as $\theta_b$ for brevity. The resulting Lagrangian horizontal velocity of the breaking wave on the free surface is denoted as $(u_\ell)_{ob}$ and is based on Eq. (50):

$$(u_\ell)_{ob} = (u_{\ell 1})_{ob} \cos\theta_b + (u_{\ell 2})_{ob} \sin\theta_b + (u_{\ell 3})_{ob} \cos 2\theta_b$$

$$+ a_b^2 k_b \sigma \frac{\cosh 2k_b h_b}{2\sinh^2 k_b h_b} . \quad (59)$$

Here $(u_{\ell 1})_{ob}$, $(u_{\ell 2})_{ob}$ and $(u_{\ell 3})_{ob}$ are exact the same as $(u_{\ell 1})_o$, $(u_{\ell 2})_o$ and $(u_{\ell 3})_o$ given in Eqs. (52) to (54) except with the following substitutions: $a = a_b$, $D = D_b$, $k = k_b$ and $h = h_b$, where the subscript $o$ represents the free surface.

Therefore, the breaker criterion can be rewritten in the following more specific form:

$$K.S.P. = \frac{(u_\ell)_{ob}}{C_b} = 1 . \quad (60)$$

This criterion, after substituting the previous Lagrangian velocity, becomes

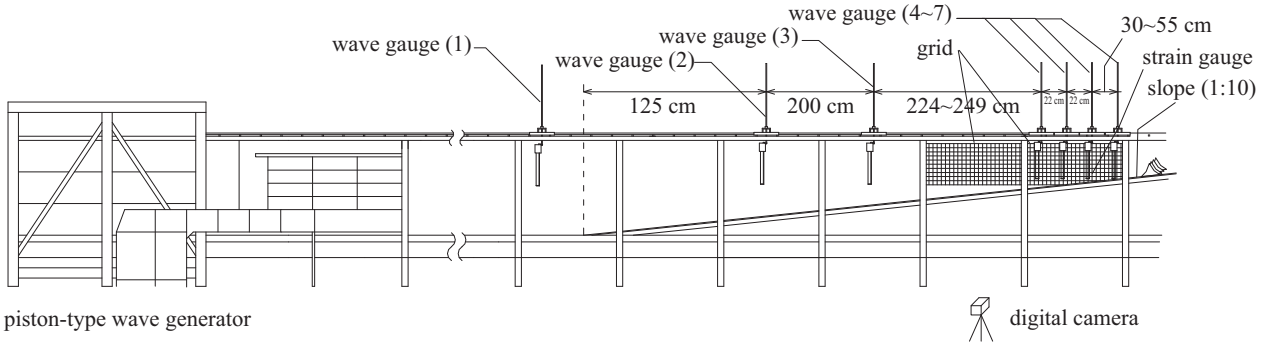


**Fig. 3. Experimental framework and instrumental setup.**

$$(\frac{k_b a_b}{\tanh k_b h_b})\cos\theta_b - \alpha a_b k_b \left[\frac{1+k_b h_b \tanh k_b h_b}{D_b^2 \tanh^2 k_b h_b}\right.$$

$$\left. + \frac{2k_b h_b + k_b^2 h_b^2 \coth k_b h_b}{D_b \sinh 2k_b h_b} - k_b h_b \coth k_b h_b - 1\right]\sin\theta_b$$

$$+ a_b^2 k_b^2 \frac{1}{\sinh^2 k_b h_b}\left[-\frac{1}{2} + \frac{3}{4}\frac{\cosh 2k_b h_b}{\sinh^2 k_b h_b}\right]$$

$$\times \cos 2\theta_b + a_b^2 k_b^2 \frac{\cosh 2k_b h_b}{2\sinh^2 k_b h_b} = 1. \quad (61)$$

According to Eqs. (49), (58) and (61), we can solve for $h_b$, $k_b$ and $\theta_b$. The maximum surface elevation $\varsigma_{\max}$, which occurs when a wave breaks, is given by

$$\varsigma_{\max} = a_b \cos\theta_b - \alpha a_b \left[\frac{k_b h_b + \tanh k_b h_b}{D_b^2 \tanh^2 k_b h_b}\right.$$

$$\left. + \frac{2k_b h_b \coth k_b h_b + k_b^2 h_b^2}{D_b \sinh 2k_b h_b} - \coth k_b h_b - k_b h_b\right]\sin\theta_b$$

$$+ \frac{3}{8} a_b^2 k_b \frac{\sinh 2k_b h_b}{\sinh^4 k_b h_b}\cos 2\theta_b . \quad (62)$$

Likewise, we can solve for the minimum breaker depth $\varsigma_{\min}$. Then, the breaker height $H_b$ is derived to be

$$H_b = (\varsigma_{\max} - \varsigma_{\min}) . \quad (63)$$

Furthermore, the breaker impulse per unit width $I_{tb}$ can be obtained using Eq. (40) and the breaker characteristics:

$$I_{tb} = (\rho \varsigma_b (u_\ell)_{ob} / k_b)(\frac{2\sinh k_b (h_b + \varsigma_b)}{\sinh k_b h_b} - 2). \quad (64)$$

Here, $\varsigma_b = \varsigma_{\max}$ .

## V. EXPERIMENTAL SETUP AND DATA ANALYSIS

The experimental measurements were conducted in a glass-walled wave tank in the Department of Marine Environment and Engineering at the National Sun Yat-sen University. This apparatus that is used for the experiment contains to following components:

(1) Wave flume: length 35 m, width 1 m, height 1.2 m. A piston-type wave generator is at one end and a wave absorber is located at the other end. Moreover, a data acquisition system, capacitance-type wave probe, strain gauge and digital camera are used.
(2) Data acquisition system: for data analysis and storage.
(3) Wave gauge: capacitance-type wave probe. (The type is MK5-3X-L100-D3. Its response time is 2 ms, and its measurement range is 0.005 m~0.45 m.)
(4) Strain gauge: transforms the wave pressure change into an electric resistance change. (The type is KFW-5-120-C1-11L3M2R. Its gage resistance is 120.4 ± 0.4 Ω; its gage factor is 2.09 ± 1.0%.)
(5) Digital camera: for imaging the wave profile during the experiments. (The type is a Casio EX-Z750, which collects images at 25 frames per second (fps).)

### 1. Experimental Setup

The experiments were conducted on a 1:10 slope. Seven wave gauges were used. The gauges were used to measure the incident wave heights and breaker heights. A strain gauge was attached to a stainless steel plate to estimate the breaking wave pressure. The waves were generated with a period of 0.8~2.0 seconds ($T_e$), a water depth of 74.3 cm ($h_e$) and wave heights of 6.0~16.0 cm ($H_e$). The experimental setup is shown in Fig. 3. The measured breaker heights ($H_b$) and breaker depths ($h_b$), and breaker impact forces ($F_{eb}$) were collected. The experimental wave progressed over a sloping bottom and approached and ultimately passed the breaking point (Fig. 4).

### 2. Experimental Breaker Impulse and Theory

(1) Theoretical estimation: The present theoretical breaker impulse per unit width ($I_{tb}$)was calculated using Eq. (64).

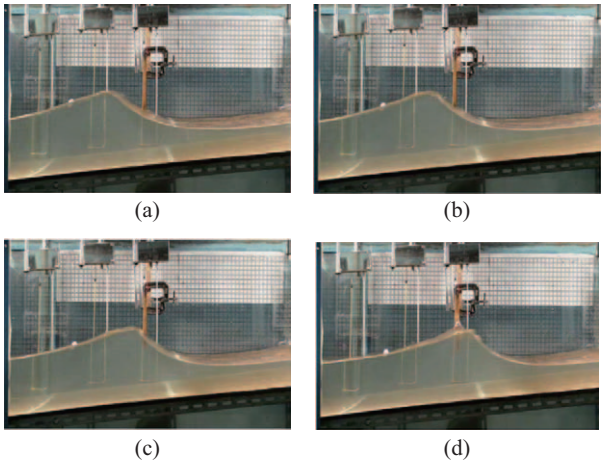


**Fig. 4. a-d Images of the experimental breaking process ($\alpha$ = 1/10) ($T_e$ = 1.4 sec, $H_e$ = 8.35 cm).**

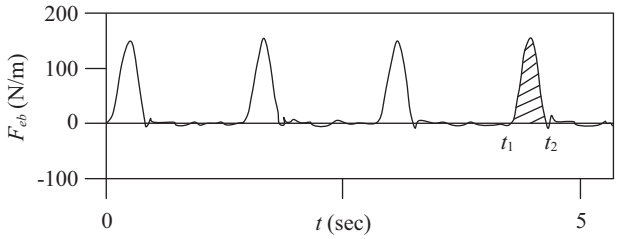


**Fig. 5. Typical breaker force at the strain gauges.**

(2) Experimental measurement: The present experimental breaker impact force was captured while the wave passed the strain gauges in the direction of wave propagation (Fig. 5). The experimental measurements included a time series of the breaker impact force that was caused by the breakers. Then, the experimental breaker impulse per unit width ($I_{eb}$) could be determined using the positive breaker force accumulation with time, e.g., from $t_1$ to $t_2$ in Fig. 5 (the oblique line area).

## 3. Theory Validation and Discussion

Many factors affect wave breaking, including the wave steepness, wave height, and bottom slope. The breaking phenomenon is extremely complicated; therefore, most previous studies provided breaker characteristics only based on experimental studies and empirical or semi-empirical formulas calibrated from laboratory data. However, the present study combined both theoretical and experimental characteristics of breaking waves. The theoretical and experimental results were compared with previously published results (Fig. 6 to Fig. 8). Fig. 7 and Fig. 8 contain the experimental results of Iwagaki et al. (1974), Deo et al. (2003), Tsai et al. (2005) and the current study. Furthermore, Fig. 9 shows the relationship between the relative breaker impulse $I^*$ and the incident wave steepness $H_0/L_0$.

Note that $I^*$ (= $I_{tb}/I_{eb}$) is the impulse ratio of the current theoretical solutions and experimental results.

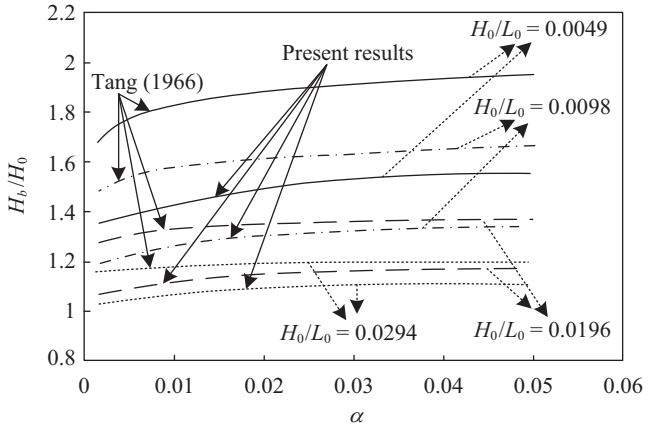


**Fig. 6. Relationship between the relative breaker height $H_b/H_0$ and the bottom slope $\alpha$.**

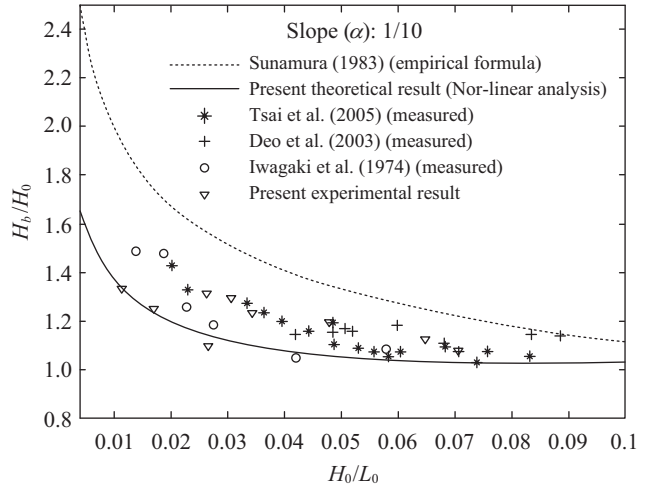


**Fig. 7. Relationship between the relative breaker height $H_b/H_0$ and the incident wave steepness $H_0/L_0$ for $\alpha$ = 1/10.**

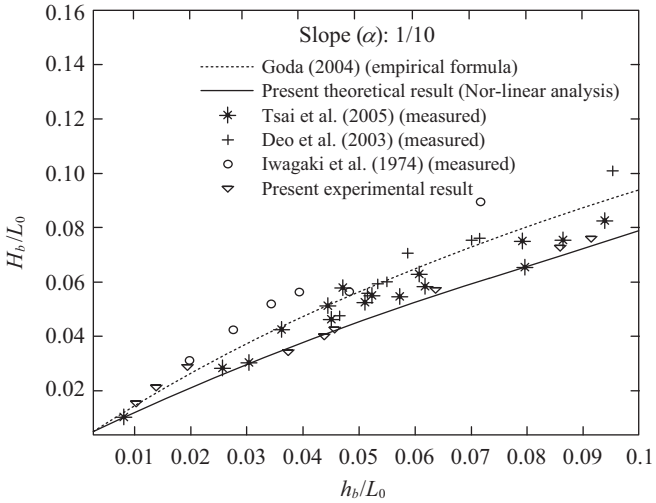


**Fig. 8. Relationship between the relative height $H_b/L_0$ and the relative depth $h_b/L_0$ for $\alpha$ = 1/10.**

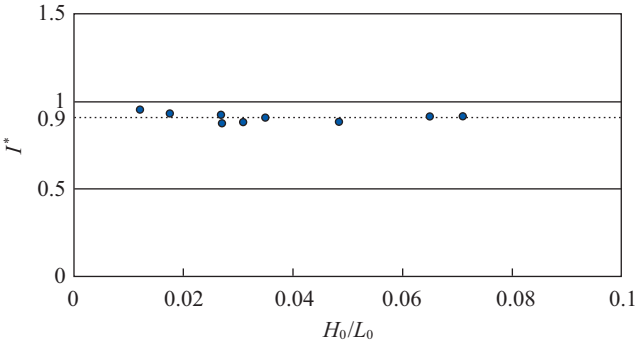


**Fig. 9. Relationship between the relative breaker impulse $I^*$ and the incident wave steepness $H_0/L_0$ for $\alpha$ = 1/10.**

Fig. 6 and Fig. 7 show that $H_b/H_0$ increases as the bottom slope increases and that $H_b/H_0$ increases as $H_0/L_0$ decreases. Moreover, $H_b/L_0$ is proportional to $h_b/L_0$, as shown in Fig. 8. Fig. 9 shows that the theoretical modeling results are consistent with the experimental data obtained in this study. Furthermore, the analytical solutions have the same trend as the previously published results and the experiment data obtained in this study (Fig. 6 to Fig. 9). The theoretical relative breaker height $H_b/H_0$, relative height $H_b/L_0$ and breaker impulse $I_{tb}$ are smaller than experimental values. This finding can be partially explained because the analysis is extended only to the second order solution in the theoretical component of this work. Accordingly, to improve the accuracy of the mathematical derivation and the present results, the analysis should be extended to a higher-order solution.

## VI. CONCLUSION

This paper provides an analytical solution for breaker characteristics and the breaker impulse because previous studies did not appropriately treat the breaker impulse. In this study, a series of experiments to measure the properties of nonlinear breaking water waves propagating over a sloping bottom were conducted in a wave tank. Then, the theoretical solutions were compared with the current experimental findings and previously published results (Fig. 6 to Fig. 9). The analytical solution was shown to exhibit the same trend as the experimental data and the previously published results. The main findings of this study are as follows:

(1) This paper provides a theoretical solution for a wave propagating over a uniformly sloped bottom from deep water to shallow water until the wave breaks. The results of this study demonstrate the characteristics and impulse of a breaking wave, which were not readily available in previously published works.
(2) A series of experiments to measure the breaker impulse were conducted in a wave tank. Good consistency was obtained by comparing the measured impulse with the theoretical value predicted using Eq. (64).
(3) The theoretical model requires only the incident wave conditions and bottom slope to determine the breaker characteristics and the breaker impulse.

## REFERENCES

Biesel, F. (1952). Study of propagation in water of gradually varying depth, U.S. National Bureau of Standards, Gravity Waves. NBS Circular 521, 243-253.

Chang, H. K. (1999). Shoaling of nonlinear waves over a gently sloping bottom. Journal of the Chinese Institute of Civil and Hydraulic Engineering 11(1), 175-180.

Chen, Y. Y., H. C. Hsu, G. Y. Chen and H. H. Hwung (2006). Theoretical analysis of surface waves shoaling and breaking on a sloping bottom. part 2: Nonlinear waves. Wave Motion 43, 339-356.

Chen, Y. Y., H. H. Hwung and H. C. Hsu (2005). Theoretical analysis of surface waves propagation on sloping bottoms, part 1. Wave Motion 42, 335-351.

Chen, Y. Y. and L. W. Tang (1992). Surface-wave propagation on gentle sloping bottom. Proc. of the 14th Ocean Engineering Conf., Taiwan, 1-22. (in Chinese)

Chen, Y. Y., B. D. Yang, L. W. Tang, S. H. Ou and J. R. C. Hsu (2004). Transformation of progressive waves propagating obliquely on gentle slope. Journal of Waterway, Port, Coastal and Ocean Engineering 130(4), 162-169.

Deo, M. C. and S. S. Jagdale (2003). Prediction of breaking waves with neural networks. Ocean Engineering 30(9), 1163-1178.

Elgar, S. and R. T. Guza (1985). Shoaling gravity waves: comparisons between field observations Linear theory and a nonlinear model. Journal of Fluid Mechanics 158, 47-70.

Galvin, C. J. (1968). Breaker type classifications of three laboratory beaches. J. Geophys Res. 73(12), 3651-3659.

Goda, Y. (1970). A synthesis of breaker indices. Trans. Japan Soc. Civil Engrs. 2(2), 227-230.

Goda, Y. (2004). A 2-D random wave transformation model with gradational breaker index. Coastal Engineering Journal 46(1), 1-38.

Gotoh, H. and T. Sakai (1999). Lagrangian simulation of breaking waves using particle method. Coastal Engineering Journal 41(3~4), 303-326.

Hansen, J. B. (1990). Periodic waves in the surf zone: Analysis of experimental data. Coastal Eng. 14(1), 19-41.

Hsiao, S. C., T. W. Hsu, T. C. Lin and Y. H. Chang (2008). On the evolution and run-up of breaking solitary waves on a mild sloping beach. Coastal Engineering 55, 975-988.

Hsieh, C. M., R. R. Hwang, M. J. Chern and W. C. Yang (2008). Using RANS to simulate breaking wave on a slopping bed. ISOPE, 684-690.

Hsieh, C. M., R. R. Hwang, Y. F. Peng, W. C. Yang and M. J. Chern (2007). Numerical simulations of solitary wave running and breaking on a slopping bed. ISOPE, 2321-2326.

Hsu, H. C., Y. Y. Chen and H. H. Hwung (2001). Surface wave propagation on a gentle sloping bottom. Proc. of the 23rd Ocean Engineering Conf., Taiwan, 33-40. (in Chinese)

Hubert, C. and J. F. Lee (1997). Plunging jet characteristics of plunging breakers. Coastal Engineering 31, 125-141.

Iwagaki, Y. and T. Sakai (1974). Tsukioka, K. and Sawai, N., Relationship between vertical distribution of water particle velocity and type of breakers on beaches. Coastal Eng. in Japan 17, 51-58.

Keller, J. B. (1958). Surface waves on water of non-uniform depth. Journal of Fluid Mechanics 4, 607-614.

Le Méhauté, B. and R. C. Y. Koh (1967). On the breaking of waves arriving at an angle to the shore. J. Hydraul. Res. 5(1), 67-88.

Li, M. S., Y. Y. Chen, H. H. Hsu and A. Torres-Freyemuth. (2013). Experimental and Lagrangian modeling of nonlinear water waves propagation on a sloping bottom. Ocean Engineering 64, 36-48.

Ogawa, Y. and N. Shuto (1984). Run-up of periodic waves on beaches of non-uniform slope. Proc. 19th Coastal Eng. Conf., ASCE, 328-334.

Rattanapitikon, W. and T. Shibayama (2000). Verification and modification of breaker height formulas. Coastal Engineering Journal 42(4), 389-406.

Saeki, H. S., A. O. Hanayasu and K. Takgi (1971). The shoaling and run-up height of the solitary wave. Coastal Engineering in Japan 14, 25-42.

Seyama, A. and A. Kimura (1988). The measured properties of irregular wave breaking and wave height change after breaking on slope. Proc. 21st Coastal Eng. ASCE, 419-432.

Street, R. L. and F. E. Camfield (1966). Observations and experiments on solitary wave deformation. Proc. 10th Conf. Coastal Eng., 284-301.

Sunamura, T. (1980). A laboratory study of offshore transport of sediment and a model for eroding beaches. Proc. 17th Coastal Eng. Conf., ASCE, 1051-1070.

Sunamura, T. (1983). Determination of breaker height and depth in the field. Ann. Rep., Inst. Geosci., Univ. Tsukuba, No. 8, 53-54.

Sunamura, T. and K. Horikawa (1974). Two-dimensional beach transformation due to waves. Proc. 14th Coastal Eng. Conf., ASCE, 920-938.

Tang, L.W. (1966). Coastal engineering researches on the western coast of Taiwan. Proc. 10th Conference on coastal Engineering, 1275-1290.

Ting, C. L., M. C. Lin, W. C. Hu and Y. H. Hsieh (2002). Reformed wave characteristics of waves breaking on a steep-sloped step. Proceedings of the 24th Ocean Engineering Conference, Taiwan, pp. 51-56. (in Chinese),

Tsai, C. P., H. B. Chen, H. H. Hwung and M. J. Huang (2005). Examination of empirical formulas for wave shoaling and breaking on steep slopes. Ocean Engineering 32, 469-483.